Target Recognition for Costal Surveillance Based on Radar Images and Generalised Bayesian Inference

Feng Ma[1, 2, 4], Yu-wang Chen[2], Xin-ping Yan[1, 3], Xiu-min Chu[1, 3*], Jin Wang[4]
[1]Intelligent Transport System Research Center, Wuhan University of Technology, P. R. China
[2]Decision and Cognitive Sciences Research Centre, the University of Manchester, UK
[3]National Engineering Research Center of Water Transportation Safety (WTS), P. R. China
[4]Liverpool Logistics, Offshore and Marine (LOOM) Research Institute, Liverpool John Moores University, UK
* xiumin_chu@126.com

Abstract: For coastal surveillance, this paper proposes a novel approach to identify moving vessels from radar images with the use of a generalised Bayesian inference technique, namely the Evidential Reasoning (ER) rule. First of all, the likelihood information about radar blips is obtained in terms of the velocity, direction, and shape attributes of the verified samples. Then, it is transformed to be multiple pieces of evidence, which are formulated as generalised belief distributions representing the probabilistic relationships between the blip's states of authenticity and the values of its attributes. Subsequently, the ER rule is used to combine these pieces of evidence, taking into account their corresponding reliabilities and weights. Furthermore, based on different objectives and verified samples, weight coefficients can be trained with a nonlinear optimisation model. Finally, two field tests of identifying moving vessels from radar images have been conducted to validate the effectiveness and flexibility of the proposed approach.

1. Introduction

Marine radar is a commonly used detection device to determine the range, altitude, direction, or speed of objects in a waterway. Normally coastlines, rocks, waves, and encountered vessels can be detected and represented as blips in frame-by-frame radar images. Compared with interactive tools such as Automatic Identification System (AIS) and Very High Frequency (VHF) radios, it is unnecessary for radar to get responses from supervised targets, and its updating rate can be much higher. Therefore, radar is considered to be a practical supervising and managing tool, especially in crowded waters. Reference [1] proposed a pre-processing approach to estimate the length of small and slow marine targets for forward scatter maritime radar. However, most marine radar systems work on a low Pulse Repetition Frequency

(PRF) mode, and the Doppler signal and velocities are ambiguous. Therefore, radar images are the kernel evidence for target extraction and recognition. A function known as automatic radar plotting aid (ARPA) is usually integrated into radar for tracking moving objects, although it often takes noises and other objects as moving vessels [2].

In fact, only a small proportion of blips are real moving vessels in crowded waters. In practice, observation angles between the radar and measured objects have significant influences on the shapes of the corresponding blips. Moreover, the centre of a blip is often different from the real centre of the corresponding object [3]. In addition, the resolutions of radar images are limited for objects at a long distance. Hence, the centres of blips are often moving in a zigzag pattern, making their trajectories different from real ones. Furthermore, many factors might block radar signals, making these trajectories discontinuous. Therefore, mistakes are easily made for identification, even by an experienced radar operator.

In practice, the identification accuracy depends on operators' experience which needs to be accumulated from long time observation. In other words, historical data is actually the evidence for manual target recognition. Inspired by this, this research proposes a probabilistic inference approach to extract moving vessels from blips in sequential radar images [4]. However, as an indispensable part of conventional probabilistic inference, the prior probability of a blip being a moving vessel is very difficult to estimate, or it even does not exist at all. This is because the number of false targets (e.g., noises or stationary objects) is affected by weather conditions, channel buildings and blocks, which can change over time, whilst the number of true targets (i.e., moving vessels) in a waterway also changes dynamically with time. Therefore, traditional probabilistic inference methods are not applicable in most cases.

In this research, the novel Evidential Reasoning (ER) rule [5] is introduced to address the above challenge. First, the attributes of blips' graphic velocity, direction, and shape (i.e., slenderness) are quantified through analysing inter-fame differences. Then, a likelihood modelling framework is proposed,

where each piece of evidence is acquired from these quantified attributes of verified samples, and is profiled as a belief distribution or a probability distribution about a blip's states being either a moving vessel or a noise. With the likelihood modelling, each piece of evidence is not relevant to the prior distribution. The ER rule is used to combine multiple pieces of evidence with the corresponding weights and reliabilities, making a conjunctive reasoning process. Furthermore, the weight of each piece of evidence can be trained from verified samples through an optimisation model under different objective settings. Finally, field testing is conducted to validate the proposed approach.

The remainder of this paper is organised as follows. In Section 2, the characteristics of radar images, typical filtering algorithms and target identification methods are reviewed. In Section 3, a novel extraction approach is presented. In Section 4, two field tests have been conducted to validate the proposed approach. The paper is concluded in Section 5.

2. Literature review

2.1 The characteristics of radar images

A pixel in a radar image normally denotes the echo intensity of a detection location. To visualise it for further processing, echo intensities are also represented as grey-scale images, or sometimes pseudo-colour images. The satellite image and the grey-scale radar image which capture the same location and surroundings of Yangtze River, Zhutuo County, Chongqing, China, are shown in Fig. 1 respectively. Through the radar image, it is easy to identify the river banks, the bridge, and the objects inside this river intuitively. Particularly, the trajectories of moving objects are generally in a zigzag pattern as discussed above. The radar position is marked as a five-pointed star in both images in Fig. 1. On the other hand, it is easy to know that an unobservable area is marked as 'Blind Area' in Fig. 1. As well as that, the shoal and rocks are represented as a series of unknown blips, which are very similar to moving vessels. Moreover, some blips caused by background noises also look like moving vessels.

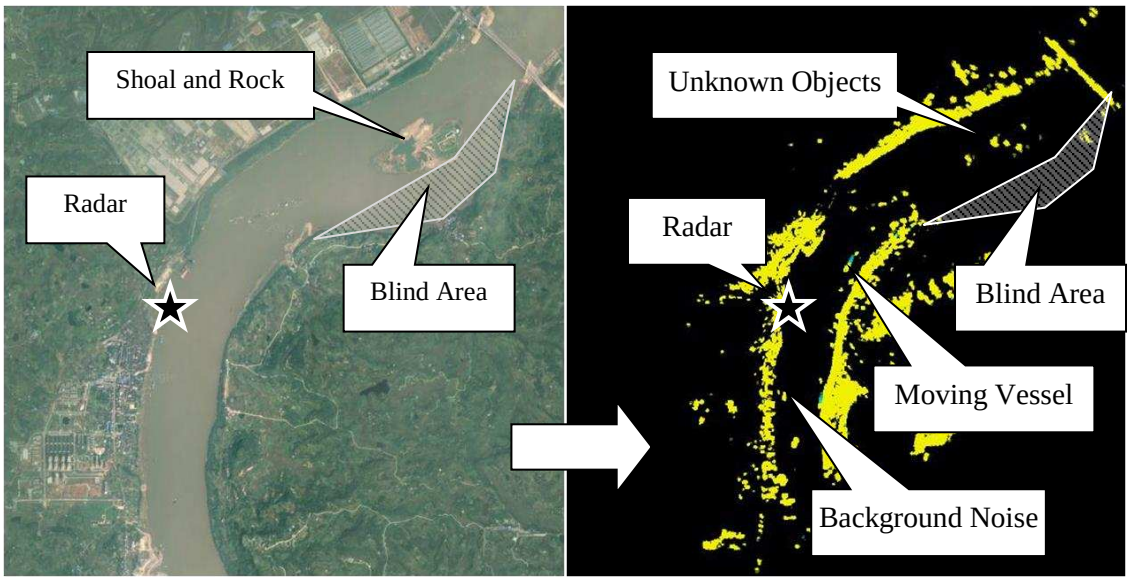

Fig. 1 The satellite and grey-scale radar images of Yangtze River, Chongqing, China

Using binarization and segmentation algorithms, a radar image can be divided into a group of colour spots or blips with different characteristics. In practice, the blips of stationary objects or noises might drift like moving vessels. In contrast, moving vessels which move slowly towards berths might also look like stationary objects or noises. Difference between moving vessels and noises might not be distinctive through looking at one single characteristic or attribute only. Therefore, it is necessary to distinguish them with the use of both observed attributes and operators' experience.

2.2 Filtering algorithms and identification methods

To address this problem, much work has been conducted generally from two perspectives. The first one is to find out the actual trajectories of blips from the zigzag ones using filtering algorithms. It is usually assumed that the deviation is caused by noise, and the real trajectory follows a different motion pattern. In light of this, an appropriate filtering algorithm might be efficient [6] [7] [8]. However, the available filtering algorithms might not be appropriate in low speed circumstances or complicated environments [9].

The other perspective is to classify radar blips or targets using pattern recognition algorithms. Particularly, non-probabilistic models are widely used. Reference [2] proposed a method to identify false

ARPA targets using fuzzy k-means (FCM). Reference [10] invented a radar target recognition method based on fuzzy optimal transformation using a high-resolution range profile. Reference [11] invented a hierarchical KNN-based vessel classifier using multi-feature joint matching for high-resolution inverse SAR images.

As discussed above, historical data is regarded as the evidence in the manual identification [12]. Therefore, probabilistic pattern recognition models might also be practicable. Typical methods include Gaussian mixture model (GMM) [13], Bayesian inference, Bayesian Network [14], Dempster's rule [15], evidence combination rules (ECRs) [16], probability box [17], and ER. The ER rule does not need the prior distribution about patterns or states, as it constitutes a likelihood modelling process. Therefore, this research aims to propose an intelligent approach to extract moving vessels from blips on the basis of the ER rule.

3. A proposed approach

3.1 Step 1: The quantifications of inter-frame differences

In fact, approximate dynamic information indicated by inter-frame differences is sufficient for manual identification. The problem is that when there are too many vessels, such a manual inspection becomes impractical. Hence, an intelligent approach of simulating the manual work will be helpful for navigational and maritime safety.

Experienced operators are able to achieve a high identification accuracy under uncertainties, because they know the regularities of moving vessels after a long term observation. For instance, the speed of a moving vessel in a specific waterway is generally stable. Therefore, a velocity indicated by a blip is a piece of direct evidence for authenticity identification. Without any filtering algorithm, it is possible to estimate the authenticity probability of a blip based on its velocity in adjacent frames. Moreover, operators can take other attributes of a blip into consideration in order to make comprehensive and accurate identification. Therefore, it is necessary to quantify these attributes.

In fact, many attributes of a blip can be taken as evidence for identification, such as velocity, course, size, colour, width, and length. However, there is a condition of using the ER rule that multiple pieces of evidence should be independent from each other. Hence, three types of evidence or attributes which are considered to be independent of each other in terms of their contributions to moving vessel identification are selected, namely, velocity, motion direction (i.e., course), and blip shape.

The velocity and motion direction can be easily understood. Real moving vessels are more likely to move with a steady velocity and a steerable course, and noise objects are more likely to drift around a small area. The velocity and motion direction can be quantified as illustrated in Fig. 2 (a) and (b). In real life, operators are generally able to identify a blip in 10 consecutive frames [2]. Therefore, this research extracts the velocity and direction attributes from the analysis of 10 frames.

Different from velocity and direction, the blip shape is more related to the imaging principle of marine radar. Visually, a moving vessel's graph is generally more slender than others, and the principle is illustrated in Fig. 2(d). In this sub-figure, a moving vessel blip possesses an afterglow, which is caused by an image delay function. This function is supported by most radar systems. The slenderness of a blip shape can be computed as the quotient of the blip's size (S_2) to the blip's circumcircle area (S_1), or S_2/S_1 in Fig. 2(c).

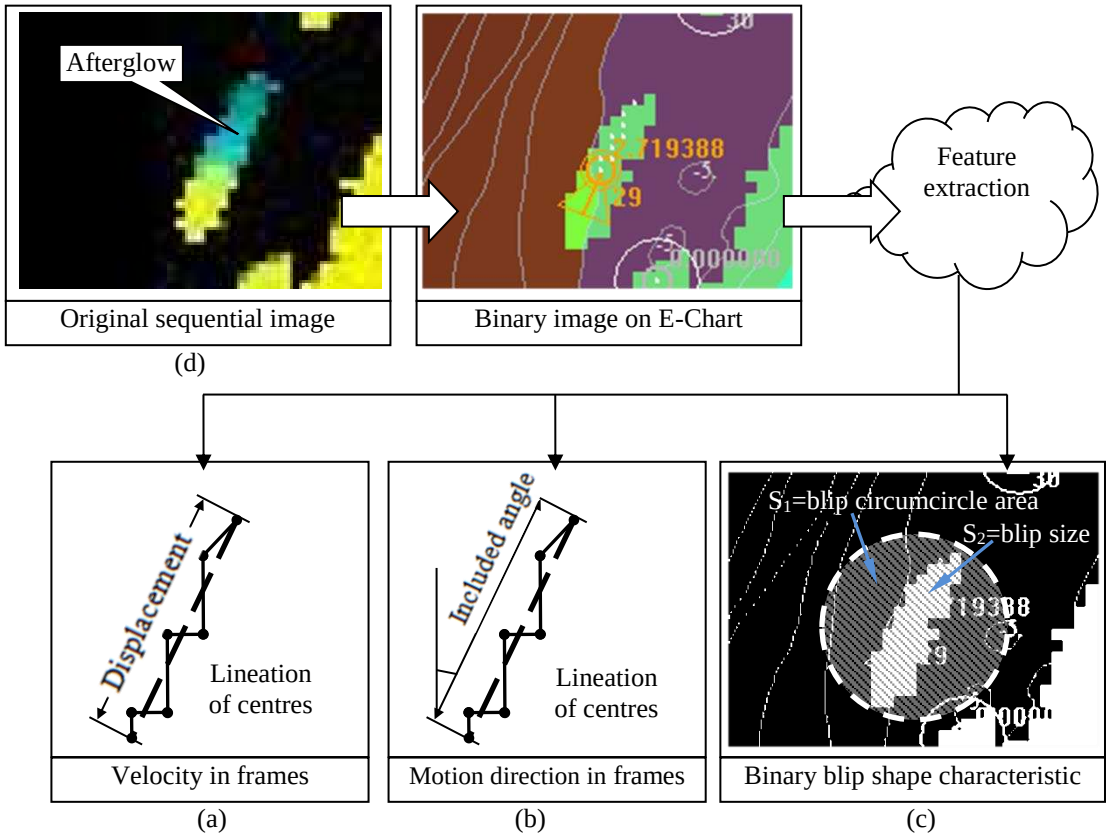

Fig. 2 *The quantification of a blip's attributes*

3.2 Step 2: Likelihood modelling and conjunctive inference using the ER rule

After the quantification of a blip's attributes, the next step is to find out their probabilistic relationships to the authenticity [18].

Suppose $\Theta = \{\theta_{True}, \theta_{False}\}$ is a set of mutually exclusive and collectively exhaustive propositions for the identification of blips, where θ_{True} is a True state and θ_{False} is a False state. Let Ø represent the empty set. The Unknown state $\theta_{Unknown}$ can be represented by the frame of discernment Θ itself. Thus, the power set of Θ consists of 4 subsets of Θ, and is denoted by 2^{Θ} or $P(\Theta)$, as follows:

$$P(\Theta) = \{\emptyset, \theta_{True}, \theta_{False}, \theta_{Unknown}\} \quad (1)$$

A Basic Probability Assignment (bpa) is a function p: $2^{\Theta} \rightarrow [0,1]$ that satisfies,

$$p(\emptyset) = 0, \sum_{\theta \subseteq \Theta} p(\theta) = 1 \quad (2)$$

where the basic probability $p(\theta)$ is assigned exactly to a proposition θ and not to any smaller subset of θ. $p(\theta)$ is generated from the values of attributes, including the velocity, direction or slenderness of a blip. Referring to the research conducted by reference [3], the likelihoods of authenticity states based on attribute values can be presented as follows.

In any verified samples shown in Table 1 [19], y_i^j denotes the frequency or the number of times that an attribute is equal to Value i for state j, with i = 1, 2, ..., L, and j = 0 for False, 1 for True, 2 for Unknown; Q^j denotes the total number of datasets for state j.

Table 1 Verified samples

States	observation attribute value of verified samples					Total
	Value 1	...	Value i	...	Value L	
False (0)	y_1^0	...	y_i^0	...	y_L^0	$Q^0 = \sum_{i=1}^{L} y_i^0$
True (1)	y_1^1	...	y_i^1	...	y_L^1	$Q^1 = \sum_{i=1}^{L} y_i^1$
Unknown (2)	y_1^2	...	y_i^2	...	y_L^2	$Q^2 = \sum_{i=1}^{L} y_i^2$

Based on Table 1, the likelihood that an attribute is equal to Value i for a state of an object is calculated in Eq. (3) and presented in Table 2 [3].

Table 2 Likelihoods without classification prior distribution

Classifications	Verified sample observation attribute value likelihood				
	Value 1	...	Value i	...	Value L
False (0)	c_1^0	…	c_i^0	…	c_L^0
True (1)	c_1^1	…	c_i^1	…	c_L^1
Unknown (2)	c_1^2	…	c_i^2	…	c_L^2

$$c_i^j = y_i^j / Q^j \quad \text{for i = 1, 2, …, L, j = 0, 1, 2.} \tag{3}$$

where c_i^j denotes the likelihood to which the attribute is expected to be equal to Value i given that state j is true.

Let p_i^j denote the probability or belief degree that an attribute with Value i points to state j, which is independent of the prior distribution about the states. p_i^j is then acquired as normalised likelihood as discussed in reference [3].

$$p_i^j = c_i^j / \sum_{k=0}^{2} c_i^k \quad \text{for i = 1, 2, …, L, j = 0, 1, 2.} \tag{4}$$

Belief distributions, given by $\{(False, p_i^0), (True, p_i^1), (Unknown, p_i^2)\}$ for i = 1, …, L, represent the probabilistic relationships between the attribute of a blip and its states. It is worth mentioning that p_i^j represents the inherent relationship between the attribute value of a blip and its states and it is not dependent on the prior distribution about the states from specific samples. For example, if a blip is moving too fast, the probability of this blip being a normal moving vessel is very low. Such a low probability or belief degree should be reflected in any reliable historical records because it is unlikely that a normal vessel could move at such an abnormal velocity.

Subsequently, a piece of evidence e_i is represented as a random set and profiled by a belief distribution (BD) as follows:

$$e_i = \{(\theta, p_i^\theta), \forall \theta \subseteq \Theta, \sum_{\theta \subseteq \Theta} p_i^\theta = 1\} \tag{5}$$

where (θ, p_i^θ) is an element of evidence e_i, representing that the evidence points to proposition (state) θ, which can be any subset of Θ or any element of $P(\Theta)$ except for the empty set, to the degree of p_i^θ, referred to as probability or degree of belief in general. (θ, p_i^θ) is referred to as a focal element of e_i if $p_i^\theta > 0$. In this occasion, p_i^θ is exactly coming from the probabilities (or belief degrees) obtained from the quantified attributes of a blip, given by Eqs. (3) and (4), where $\theta = 0(False), 1(True)$ or $2(Unknown)$.

In addition, a reliability is associated with evidence e_i, denoted by r_i, which represents the ability of the information source to provide correct assessment or solution for a given problem [18]. On the other hand, evidence e_i can also be associated with a weight, denoted by w_i. The weight of evidence can be used to reflect its relative importance in comparison with other evidence and can be determined according to the one who uses the evidence.

To combine a piece of evidence with another piece of evidence, it is necessary to take into account three elements of the evidence: its belief distribution, reliability and weight. In the ER rule, this is achieved by defining a so-called weighted belief distribution with reliability as follows:

$$m_i = \{\left(\theta, \widetilde{m}_{\theta,i}\right), \forall \theta \subseteq \Theta; (P(\Theta), \widetilde{m}_{P(\Theta),i})\} \tag{6}$$

where $\widetilde{m}_{\theta,i}$ measures the degree of support for θ from e_i with both the weight and reliability of e_i taken into account, defined as follows:

$$\widetilde{m}_{\theta,i} = \begin{cases} 0 & \theta = \phi \\ c_{rw,i} m_{\theta,i} & \theta \subset \Theta, \theta \neq \phi \\ c_{rw,i}(1 - r_i) & \theta = P(\Theta) \end{cases} \tag{7}$$

$$c_{rw,i} = 1/(1 + w_i - r_i) \tag{8}$$

where $c_{rw,i}$ denotes a normalisation factor, and the degree of support $m_{\theta,i}$ for proposition (state) θ from evidence i is given by $m_{\theta,i} = w_i p_i^{\theta}$, with p_i^{θ} being the degree of belief that evidence i points to θ. As described previously, p_i^{θ} can be obtained using Table 1, Table 2, Eqs. (2) and (3). $P(\Theta)$ is the power set of the frame of discernment Θ that contains all mutually exclusive hypotheses.

If every piece of evidence is fully reliable, i.e., $r_i = 1$ for any i, the ER rule reduces to Dempster's rule [20]. In this research, such pieces of evidence are not fully reliable, or $r_i < 1$. The combination of two pieces of evidence e_1 and e_2 defined in Eq. (5) will be conducted as follows:

$$p_{\theta,e(2)} = \begin{cases} 0 & \theta \subseteq \phi \\ \frac{\widehat{m}_{\theta,e(2)}}{\sum_{D \subseteq \Theta} \widehat{m}_{D,e(2)}} & \theta \subseteq \Theta \end{cases} \tag{9}$$

$$\widehat{m}_{\theta,e(2)} = \left[(1 - r_2) m_{\theta,1} + (1 - r_1) m_{\theta,2}\right] + \sum_{B \cap C = \theta} m_{B,1} m_{C,2} \tag{10}$$

where $m_{\theta,1}$, $m_{\theta,2}$ $m_{B,1}$ and $m_{C,2}$ are given by Eqs. (6), (7) and (8); B, C and D denote any element in the power set $P(\Theta)$ except for empty set; $p_{\theta,e(2)}$ is the synthetic belief degree to proposition (state) θ when taking both pieces of evidence, e_1 and e_2 into consideration. Reference [4] proved that the belief degree

here is equivalent to the probability in Bayes' rule if each belief degree is assigned to a single state only and p_i^{θ} is calculated by Eq. (5).

3.3 Step 3: Nonlinear optimisation on weight coefficients

The reliability and weight of evidence can be obtained in the following discussion. Referring to the radar design requirement [2], 95% of marine radar observations are credible in common scenarios. Since all the sequential images come from the same radar sensor, 0.95 can be considered as the value of reliability for all evidence in the first place. As described previously the weight of a piece of evidence reflects its relative importance, and in practice, such importance is exactly related to verified samples and the specific optimisation objective [21].

A typical objective is to maximize the global accuracy of identification. For simplicity, the global accuracy can be considered as the sum of all the output belief degrees (probabilities) that have been assigned to the correct propositions (states). In fact, the global accuracy generally includes judgments on objects. Thus, a Boolean function is often used to determine a discrete state (usually True or False state) of objects based on their belief distributions (probability distributions) of the corresponding hypotheses. However, the Boolean function is very difficult to be modelled using optimisation algorithms [21]. Hence, the weight can only be solved in a compromised way as follows.

Let $Vessel = \{V_1,\ V_2,\ \cdots,\ V_m\}$, $Noise = \{N_1,\ N_2,\ \cdots,\ N_n\}$ be the verified observations from moving vessels and noises (or stationary objects) respectively. For a noise observation N_j, $p_{\theta_1,e}(N_j, w^T)$ denotes the belief degree or probability of proposition (state) θ_1, where $\theta_1 = 0(False)$. Similarly, for an observation from a moving vessel V_i , $p_{\theta_2,e}(V_i, w^T)$ denotes the belief degree or probability of proposition (state) θ_2 , where $\theta_2 = 1(True)$. $p_{\theta_1,e}(N_j, w^T)$ and $p_{\theta_2,e}(V_i, w^T)$ are obtained with the conjunctive reasoning process using the ER rule. $p_{\theta_1,e}(N_j, w^T)$ and $p_{\theta_2,e}(V_i, w^T)$ share the same weight vector $w^T = \{w_1, w_2, w_3\}$, which denotes the weights of velocity, course and shape evidence. Hence, the global

accuracy or sum of inferred probabilities that have been assigned to the correct propositions (states) is presented as,

$$\phi(w^T) = \sum_{j=1}^{n} p_{\theta_1,e}(N_j, w^T) + \sum_{i=1}^{m} p_{\theta_2,e}(V_i, w^T) \quad (11)$$

The appropriate w^T should make $\phi(w^T)$ maximum. Therefore, the optimisation formulation can be presented as,

$$w^T = \arg \max_{w^T:feasible} \phi(w^T) \quad (12)$$

As discussed above, only a compromised solution of weights can be obtained through the optimisation model without a Boolean function. Since Eq. (11) is continuous and derivable, the appropriate weights of pieces of evidence can be obtained with the '*fmincon'* function of MATLAB [21]. Particularly, the weights of pieces of evidence can also be set through optimising specific objectives, depending on the requirements. Other optimisation objectives will be discussed in the following case study.

4. A case study

To validate the proposed approach, one field test was conducted in Zhuotuo County, Yongchuan, Chongqing, China from 11:55:36 to 16:05:35 on the 11th January 2015, when the weather was fine. To validate the flexibility of the proposed approach, another field test has been conducted in a windy and rainy weather for comparison from 9:30:00 to 13:32:05 on the 19th July, 2017. In such weather, the waves were high, and the noise signals increased significantly.

4.1 Experiment platform

The photograph of the experiment platform is shown in Fig. 3, and the testing radar is installed on a wharf boat. During the first test, it provided 5808 sequential radar images. A typical radar image is presented in Fig. 1. In total, 718 suspected vessel blips have been captured. During the experiment, there were 42 vessels passing through the waterway. In four hours, there were 212,944 individual observations (i.e., blips) identified. However, only 8,143 observations were from moving vessels. It is worth

mentioning that the width of the waterway is only about 100 meters, therefore these blips can be validated by visual inspections.

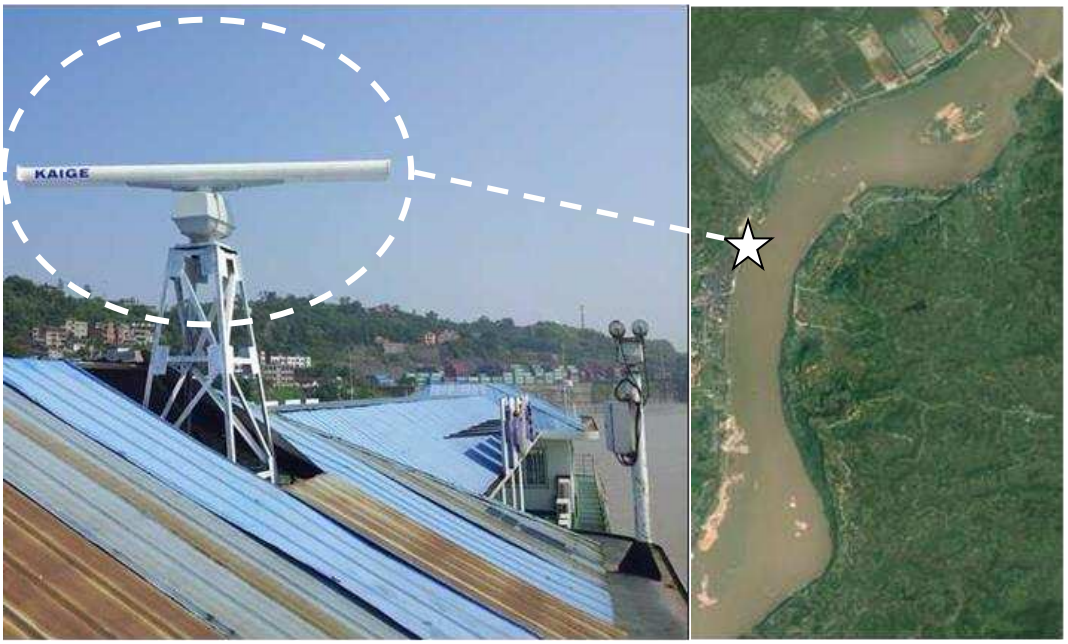

Fig. 3 Experiment Radar at Zhutuo County, Yongchuan, Chongqing, China

Eventually, the verified samples have been divided into three sets by time. The samples from the first two hours are used to model the correlations between quantified attributes and the probabilities about states as discussed in Sections 3.1 and 3.2; the ones from the third hour are used to train the weight coefficients; the rest are used for a global validation.

4.2 Step 1: Attribute quantification

The first step is to quantify inter-frame differences and graphic attributes of blips. A software program complied by VC++ has been developed and presented as shown in Fig. 4. The binarization and segmentation have been conducted. The radar images have already been overlaid on the S57 (which is the map format defined by the International Maritime Organization) electronic chart of the waterway, which are easy to understand. Three typical verified objects, two noise objects No.17, No.14, and one vessel object No.29, were notified as the red squares, and the enlarged images are also included in Fig. 4. The white circles and orange circles are the objects' labels. The centres of the objects are also marked

accordingly. Especially, the white dots are the former centres of the objects. Intuitively, the moving vessel objects are different from noises in terms of the attributes of the velocity, course, and graphic shape.

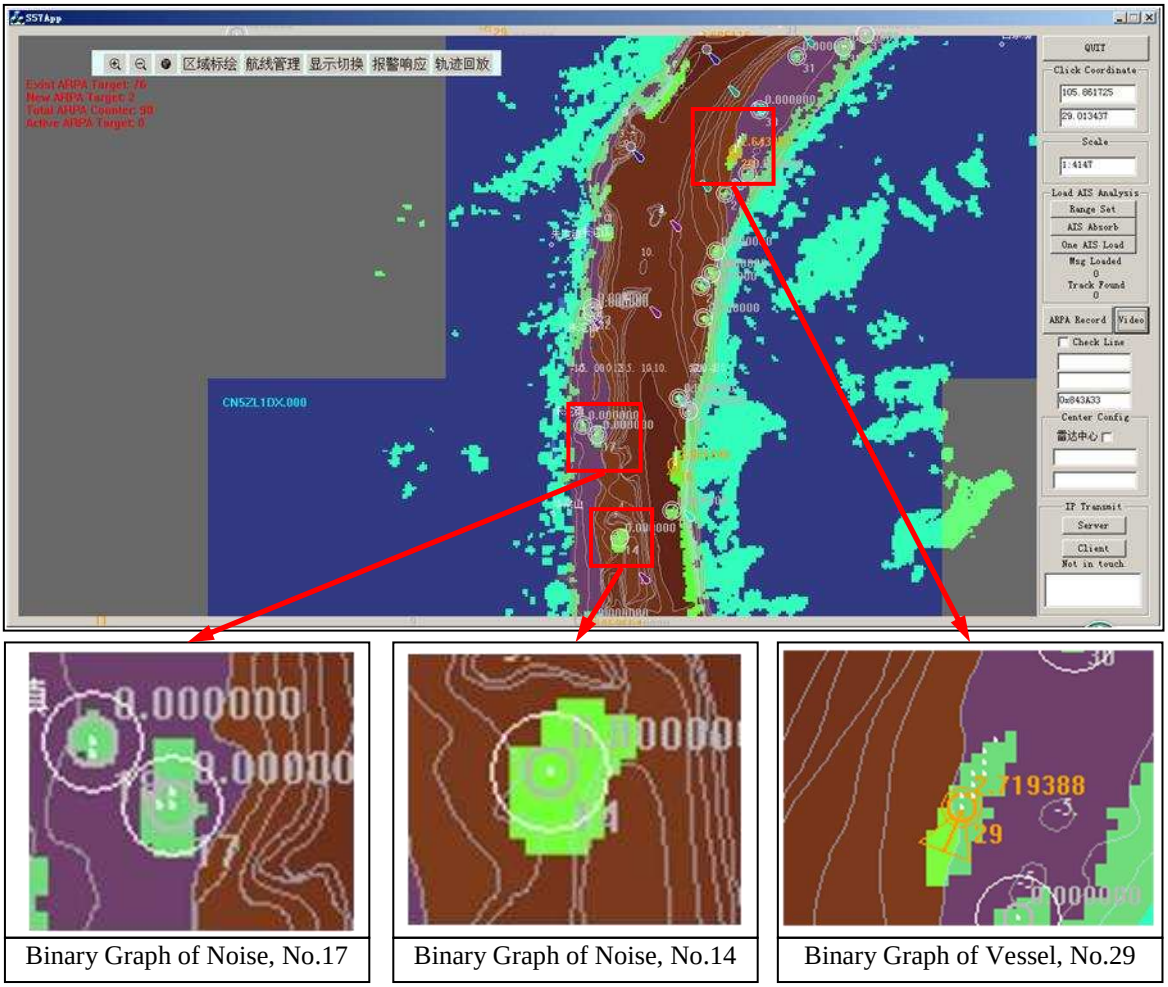

Binary Graph of Noise, No.17 | Binary Graph of Noise, No.14 | Binary Graph of Vessel, No.29

Fig. 4 The VC++ analysis software and demonstrative objects

Using the software program, all the blips in sequential images have been transformed to verified records presented in a text form with discrete values. A typical record is presented in Fig. 5. The record contains several fields, which are separated by commas and represent different types of discrete attribute values. In this way, the course (direction), velocity, and slenderness are all stored in one record. Moreover, the verified vessel and noise records are saved separately.

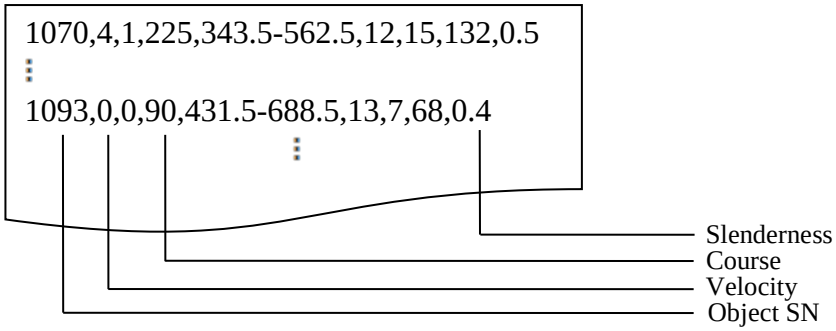

Fig. 5 Text record definitions

4.3 Step 2: Evidence modelling and targets extraction

All the blip samples have been transformed to text forms shown in Fig. 5. Using the 106,473 verified samples from the first two hours of the experiment described in Section 4.1, the relationships between attribute values and probabilities of being moving vessels or noises can be obtained as follows.

In this case study, there are only two kinds of blips captured, True state (moving vessels) and False state (noises or stationary objects). No blips with the Unknown state have been captured. Taking the velocity of 4 pixels per 10 frames as an example, it is the 5th value in the velocity attribute. In the 102,310 False state samples, 1,672 records with this velocity have been found. In the 4,163 True state samples, 1,172 records with this velocity have been found. Based on the velocity and Eq. (3), the likelihoods of the corresponding blip being at the True and False states are presented as,

$$c_5^0 = y_5^0/Q^0 = \frac{1672}{102310} = 0.0163 \quad (13)$$

$$c_5^1 = y_5^1/Q^1 = \frac{1172}{4163} = 0.2815 \quad (14)$$

Fig. 6 presents the likelihoods of the True and False states based on the velocity, where the X axis represents the velocity, and the Y axis represents the likelihoods based on Eq. (3).

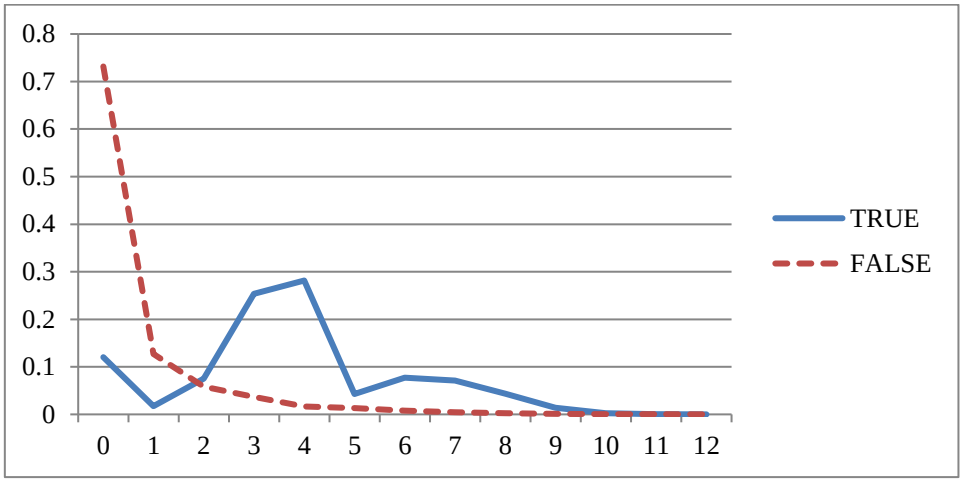

Fig. 6 Velocity-based likelihoods

As no blip with the Unknown state has been captured in this experiment, according to Eq. (4), the normalised likelihoods or probabilities of this blip being at the True state and False state can be presented as,

$$p_5^0 = c_5^0/(c_5^0 + c_5^1) = 0.0547 \quad (15)$$

$$p_5^1 = c_5^1/(c_5^0 + c_5^1) = 0.9453 \quad (16)$$

In this case, $p_5^2 = 0$. Using this procedure, for any velocity value, the probabilities or belief degrees of each state (True, False, or Unknown) can be obtained using Eq. (4). Figs. 7 and 8 present the likelihoods of the True and False states based on the slenderness and course, where the X axis represents the slenderness or course, the Y axis represents the likelihoods based on Eq. (3).

Overall, vessel blips (True state) are more slender than noises (False state) as shown in Fig. 7. It is worth noting that a slenderness value is continuous, and the interval of 0.1 is considered to be sufficient to describe it accurately. The size of a blip is based on how many pixels it is occupying. Therefore, when a blip is too small, there is a chance that a slenderness value is larger than 1. As shown in Fig. 8, the course of noises (False state) crowds on 0, 45, 90, 135, 180, 225, 270 and 315 degrees. On contrary, the course of moving vessels (True state) crowds on the major directions of the waterway.

Then, the probabilities about authenticity states based on slenderness and course can also be obtained using these samples and Eq. (4). In other words, the velocity, course and slenderness evidence can be obtained with this procedure.

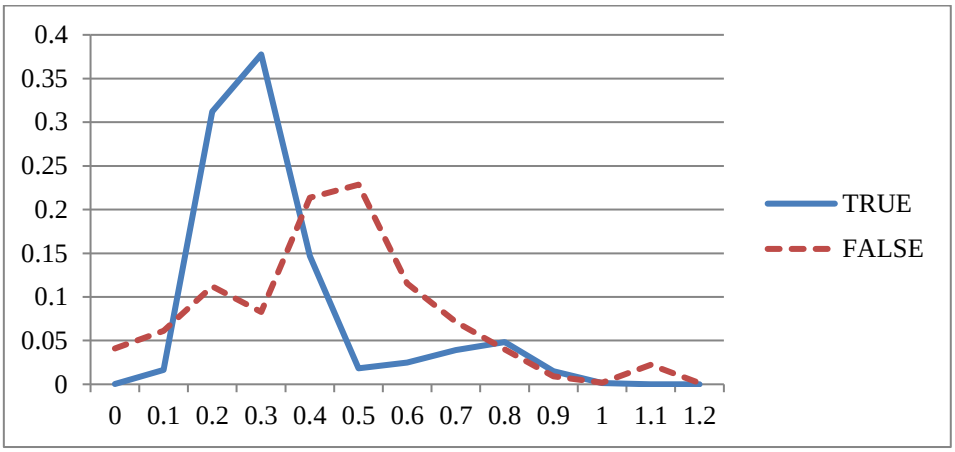

Fig. 7 Shape/Slenderness-based likelihoods

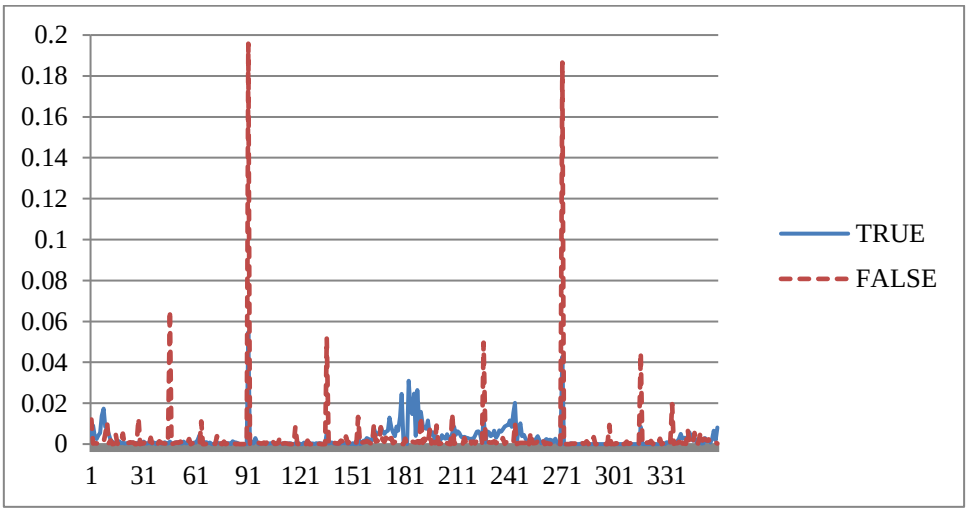

Fig. 8 Direction-based likelihoods

Eventually, these pieces of evidence can be combined using the ER rule with corresponding weights and reliabilities, as discussed in Section 3.2. The reliability and weight coefficients of a piece of evidence should be equal when there is no verified sample or a specific optimisation objective [18]. In this occasion, reliability and weight can be considered as 0.95 for all the evidence as described in Section 3.3. Then the probabilities of each blip being at the True state can be calculated, and an example is presented in Appendix.

As mentioned in Section 4.1, the verified samples captured in the last hour of the first experiment are used for a global validation. In practice, 50% is an intuitive and reasonable threshold. In other words, if the reasoning probability of a blip being the True state is larger than 50%, the blip (observation) is considered as a moving vessel. Otherwise, it can be considered as a noise or stationary object. Overall, the identification results in the fine and rainy weather are presented in Table 3.

Table 3 Results of analysis of the verified samples using the developed model, when $\{w_1, w_2, w_3\} = \{0.9500, 0.9500, 0.9500\}$

		Total	Correct identification	In-correct identification	Accuracy
Fine Weather	Moving vessel	2,082	1,700	382	81.65%
	Noises or stationary objects	51,156	47,712	3,444	93.27%
	Overall	53,238	49,412	3,826	92.81%
		Total	Correct identification	In-correct identification	Accuracy
Windy Rainy Weather	Moving vessel	1,156	956	200	82.69%
	Noises or stationary objects	83,355	75,853	7,502	90.09%
	Overall	845,11	76,809	7,702	90.08%

In total, there are 2,082 verified observations of being moving vessels and 51,156 verified observations of being noises or stationary objects in the analysis. As for the verified observations (blips) of being moving vessels, the developed model produced 1,700 correct identifications out of 2,082 observations, leading to the identification accuracy of 81.65%. As for the 51,156 verified observations of being noises or stationary objects, the model produces the identification accuracy of 93.27%. The global identification accuracy is 92.81%, and the ER rule turns out to be efficient. The results in windy and rainy weather are similar. It is worth noting that mistakes are easily made by experienced operators [22].

In fact, the risk levels caused by each type of misjudgement (e.g. taking a moving vessel as a noise) are different. To take a moving vessel as a noise is more harmful since it could cause an accident.

4.4 Step 3: Weight coefficient training

To make the identification more practical, appropriate weight coefficients can be trained with a specific objective and verified samples as discussed in Section 3.3. With the verified samples gathered in the third hour of the experiment, weight coefficients can be obtained based on Eq. (12). As described, the optimisation based on Eq. (12) is aiming to make the global identification accuracy maximised.

Particularly, such a procedure can be implemented by the '*fmincon'* function of MATLAB, and the appropriate weights are obtained as $w^{T*} = \{w_1, w_2, w_3\} = \{1.000, 1.000, 1.000\}$ when in fine weather. w^{T*} is then used as the weight vector for the verified samples of the last hour. The same procedure has been conducted on the samples collected in rainy and windy weather. The results obtained are presented in Table 4.

Table 4 Results of analysis of the verified samples using the developed model, when $\{w_1, w_2, w_3\} = \{1.000, 1.000, 1.000\}$ in fine weather and $\{w_1, w_2, w_3\} = \{1.000, 1.000, 1.000\}$ in rainy and windy weather.

		Total	Correct identification	In-correct identification	Accuracy
Fine Weather	Moving vessel	2,082	1,684	434	79.20%
	Noises or stationary objects	51,156	48,184	3,444	94.19%
	Overall	53,238	49,868	3,878	93.67%
		Total	Correct identification	In-correct identification	Accuracy
Windy Rainy Weather	Moving vessel	1,156	902	254	78.03%
	Noises or stationary objects	83,355	79,187	4,168	95.00%
	Overall	845,11	80,089	4,422	94.77%

According to Table 4, although the global identification accuracy increases to 93.67%, the identification accuracy of observations from moving vessels slightly decreases. Therefore, another optimisation objective is considered, which is to lower the frequency of taking moving vessel targets as noises. Based on the same principle discussed in Section 3.3, such an objective can be formulated as,

$$\phi'(w^T) = \sum_{i=1}^{m} p_{\theta,e(3)}(V_i, w^T) \tag{17}$$

where $\theta = 1(True)$, $p_{\theta,e(3)}$ denotes the belief degree or probability of proposition (state) θ, obtained through the ER rule-based conjunctive reasoning process with the three pieces of evidence considered in this research. V_i and w^T have been defined in Eq. (11). Taking the verified samples from the third hour of the first experiment as the training set, the optimisation function is updated as,

$$w^T = \arg \max_{w^T:feasible} \sum_{i=1}^{m} p_{\theta,e(3)}(V_i, w^T) \tag{18}$$

Using the '*fmincon'* of MATLAB 2013b, $w^{T*} = \{w_1, w_2, w_3\} = \{1.000, 0.002, 1.000\}$ in fine weather. Subsequently, for the verified samples from the last hour, the results are presented in Table 5. The same procedure has been conducted on the samples in rainy and windy weather. The corresponding results are also presented in Table 5.

Table 5 Results of analysis of the verified samples using the developed model, when $\{w_1, w_2, w_3\} = \{1.000, 0.002, 1.000\}$ in fine weather and $\{w_1, w_2, w_3\} = \{1.000, 0.1972, 1.000\}$ in rainy and windy weather.

		Total	Correct identification	In-correct identification	Accuracy
Fine Weather	Moving vessel	2,082	1,738	344	**83.48%**
	Noises or stationary objects	51,156	46,626	4,530	90.36%
	Overall	53,238	48,364	4,874	90.09%
		Total	Correct identification	In-correct identification	Accuracy
Windy Rainy Weather	Moving vessel	1,156	961	195	**83.13%**
	Noises or stationary objects	83,355	73,352	10,003	88.00%
	Overall	84,511	74,313	10,198	87.93%

As indicated in Table 5, although the global identification accuracy decreases to 90.09%, the identification accuracy of moving vessel blips is improved to 83.48%. Such an identification model may be preferred by radar operators. It can be noted that the course evidence has been almost eliminated after this optimisation. The results in windy and rainy weather are similar. Compared with Tables 3 and 5, the results in Table 4 are less practical for use.

For comparison, the error back-propagation (BP) based artificial neural network (ANN) and Bayesian Networks (BN) are introduced to process the same samples [23]. For simplicity, the neural pattern recognition tool (nprtool) of MATLAB 2013b is used to implement the classification of BP-based ANN and BN (KrishnaSri et al., 2016). Generally, the element number of the hidden layer of ANN is set to be twice the number of the input elements, including velocity, course, and slenderness [23], which is 6 in this research. The recognition process of BN will follow the procedure of [24]. The same as the proposed approach, the first half of the verified samples are used for training the coefficients of ANN and BN, and the rest are used for validation. Different from the proposed approach, 0.5 or 50% is not an appropriate threshold in an ANN or BN model. A receiver operating characteristic (ROC) curve is widely used to obtain a threshold, which can also be implemented with nprtool of MATLAB. With the help of ROC, the detailed recognition result is presented in Tables 6 and 7. In particular, the recognition accuracy of ANN on real moving vessels is only 63.59%. Given the significance of identifying moving vessels from the blips on a radar screen, the recognition process is less impressive in this occasion. The recognition

accuracy of BN is very close but still lower than the proposed approach, especially in rainy and windy weather. Overall, the proposed approach incorporating the ER rule is superior.

Table 6 Results of analysis using BP-based ANN

		Total	Correct identification	In-correct identification	Accuracy
Fine Weather	Moving vessels	2,082	1,324	758	**63.59%**
	Noises or stationary objects	51,156	49,109	2,047	96.00%
	Overall	53,238	50,433	2,805	94.73%
		Total	Correct identification	In-correct identification	Accuracy
Windy Rainy Weather	Moving vessel	1,156	640	516	**55.36%**
	Noises or stationary objects	83,355	76,685	6,670	92.00%
	Overall	84,511	77,325	7,186	91.50%

Table 7 Results of analysis using Bayesian Networks

		Total	Correct identification	In-correct identification	Accuracy
Fine Weather	Moving vessels	2,082	1,324	758	**83.14%**
	Noises or stationary objects	51,156	49,964	1,190	90.08%
	Overall	53,238	51,288	1,948	90.03%
		Total	Correct identification	In-correct identification	Accuracy
Windy Rainy Weather	Moving vessel	1,156	868	288	75.09%
	Noises or stationary objects	83,355	70,851	12,504	85.00%
	Overall	84,511	71,719	12,792	84.86%

5. Conclusions and Discussions

The paper proposed an ER rule-based approach to identify blips using sequential radar images and verified samples for coastal surveillance. The main contributions and conclusions are given below.

1) The approach is based on original sequential radar images which contain sufficient information for target extraction. Different from traditional filtering algorithms, it does not make any assumption on objects' states.

2) After appropriate quantifications on inter-frame differences of blips, likelihoods of states can be obtained using verified samples. Subsequently, these pieces of evidence can be combined using the ER rule.

3) With a specific objective set, weight coefficients of three attributes for synthesis can be trained in a nonlinear optimisation model.

Overall, the proposed approach can deliver the identification accuracy of over 90%. It can also be used in situations where the behaviours of moving vessels need to be further investigated for safety and

security reasons. In the future research, the quantification of blip attributes should be conducted in fewer frames to improve the recognition speed. Moreover, the improved approach should be capable of distinguishing rocks, shoals from background noises. The continuities of blips may need to be introduced into the conjunctive inference, and it might further improve the identification accuracy.

6. Acknowledgements

Thanks for the financial support given by National Science Foundation of China (Grants no. 61503289), Royal Society (Grant no. IE140302), EU FP6 (Grant no. MC 314836), Hubei Province Natural Science Foundation (Grant no. 2013CFA007), and Information Foundation of Ministry of Transport of the People's Republic of China (Grant no. 2013-364-548-200).

7. References

[1] Kabakchiev, H., Behar, V., Garvanov, I., Kabakchieva, D., Daniel, L., Kabakchiev, K. & Cherniakov, M: 'Experimental Verification of Maritime Target Parameter Evaluation in Forward Scatter Maritime Radar', IET Radar, Sonar & Navigation, 2014, 9(4), 355-363.

[2] Ma, F. Wu, Q. Yan, X. Chu, X. & Zhang, D.: 'Classification of Automatic Radar Plotting Aid Targets Based on Improved Fuzzy C-Means', Transportation Research Part C: Emerging Technologies, 51, 180-195.

[3] IEC I. 62388: 'Maritime Navigation and Radio-communication Equipment and Systems, Shipborne Radar. Performance Requirements, Methods of Testing and Required Test Results', 2013.

[4] Faruq, A., Abdullah, S. S., Fauzi, M. & Nor, S.: 'Optimization of depth control for unmanned underwater vehicle using surrogate modeling technique', IET Intelligent Transport Systems, 2011, 5(3), 197-206.

[5] Yang, J. B. & Xu, D. L.: 'A Study on Generalising Bayesian Inference to Evidential Reasoning', In Belief Functions: Theory and Applications, Yang, J. B., Xu, D. L. & Cuzzolin, F. (ed.), 2004, 180-189.

[6] Farrell, W. J.: 'Interacting Multiple Model Filter for Tactical Ballistic Missile Tracking', IEEE

Transactions on Aerospace and Electronic Systems, 2008, 44(2), 418-426.

[7] Yoo, J. C. & Kim, Y. S.: 'Alpha–beta-tracking Index (α–β–Λ) Tracking Filter. Signal Processing, 2003, 83(1), 169-180.

[8] He, X. Bi, Y.& Guo, Y.: 'Target Tracking Algorithm of Ballistic Missile in Boost Phase Based on Ground-based Radar Systems', Journal of Information & Computational Science, 2015, 12(2), 855–864.

[9] IEC I. 62288: 'Maritime Navigation and Radio-communication Equipment and Systems - Presentation of Navigation-related Information on Shipborne Navigational Displays - General Requirements, Methods of Testing and Required Test Results', 2014.

[10] Zhou, D. Shen, X. & Yang, W.: 'Radar Target Recognition Based on Fuzzy Optimal Transformation Using High-resolution Range Profile', Pattern Recognition Letters, 2013, 34(3), 256-264.

[11] Zhao, X. Wang, S. Zhang, J. Fan, Z.& Min, H.: 'Real-time Fault Detection Method Based on Belief Rule Base for Aircraft Navigation System', Chinese Journal of Aeronautics, 2013, **26**, (3), pp. 717-729.

[12] Lee, D. J.: 'Automatic Identification of ARPA Radar Tracking Vessels by CCTV Camera System', Journal of the Korean Society of Fisheries Technology, 2009, 45(3), 177-187.

[13] Xia, Y. Shi, X. Song, G. Geng, Q. & Liu, Y.: 'Towards Improving Quality of Video-Based Vehicle Counting Method for Traffic Flow Estimation', Signal Processing, 2016, 120(c), 672-681.

[14] Zhang, D. Yan, X. P. Yang, Z. L. Wall, A.& Wang, J.: 'Incorporation of Formal Safety Assessment and Bayesian Network in Navigational Risk Estimation of the Yangtze River', Reliability Engineering & System Safety, 2013, 118, 93-105.

[15] Li, B. & Pang, F. W.: 'an Approach of Vessel Collision Risk Assessment Based on the D–S Evidence Theory', Ocean Engineering, 2013, 74, 16-21.

[16] Smarandache, F., Dezert, J. & Tacnet, J.: 'Fusion of Sources of Evidence with Different Importances

and Reliabilities', Proceedings of 13th Information Fusion (FUSION) Conference, 26-29 July 2010, Edinburgh, UK, 1-8.

[17] Sun, S. Fu, G. Djordjević, S. & Khu, S. T.: 'Separating Aleatory and Epistemic Uncertainties: Probabilistic Sewer Flooding Evaluation Using Probability Box', Journal of Hydrology, 2012, 420, 360-372.

[18] Yang, J. B. & Xu, D. L.: 'ER Rule for Evidence Combination', Artificial Intelligence, 2013, 205, 1-29.

[19] Xu, X.B. Zhou, Z. & Wang, C. L.: 'Data Fusion Algorithm of Fault Diagnosis Considering Sensor Measurement Uncertainty', International Journal on Smart Sensing and Intelligent System, 2013, 6(1), 171-190.

[20] Dempster, A. P.: 'Upper and Lower Probabilities Induced by a Multivalued Mapping', The Annals of Mathematical Statistics, 1967, 325-339.

[21] Nguyen, T. & Sanner, S.: 'Algorithms for Direct 0--1 Loss Optimisation in Binary Classification', Proceedings of the 30th International Conference on Machine Learning, 16-21 June 2013, Atlanta, Georgia, USA, 1085-1093.

[22] Lin, B. & Huang, C. H.: 'Comparison between ARPA Radar and AIS Characteristics for Vessel Traffic Services', Journal of Marine Science and Technology, 2006, 14(3), 182-189.

[23] Schmidhuber J.: 'Deep Learning In Neural Networks: An Overview', Neural Network, 2015; 61, 85-117.

[24] Ma, F., Chen, Y. W., Yan, X. P., Chu, X. M. & Wang, J: 'A Novel Marine Radar Targets Extraction Approach based on Sequential Images and Bayesian Network', Ocean Engineering, 2016, 120, 64-77.

Appendix

Taking the record "178,12,4,135,549.5-479.5,5,11,33,0.3" as an example, its probabilities of states can be obtained as follows. According to the definition of sentence given by Section 4.2, the attribute values of the corresponding blip can be obtained as, "serial number: 178", "velocity: 12 pixel in 10

frames", "direction (course): 135 degree", "slenderness: 0.3". Then, based on the velocity, course, and slenderness evidence modelling in Section 4.2, three pieces of evidence can be obtained and shown in Table 6. The weights and reliabilities are set to be 0.95.

Table 6 Three pieces of evidence

	Belief degrees (probabilities) to $\{\theta_{False}, \theta_{True}, \theta_{unknown}\}$	Reliability	Weight
Velocity	{0.4351, 0.5649, 0}	0.95	0.95
Course (Direction)	{0.3654, 0.6346, 0}	0.95	0.95
Slenderness	{0.0261, 0.9739, 0}	0.95	0.95

Using Eqs. (7), (8), (9) and (10), such pieces of evidence can be combined, and the result is presented as $\{p(\theta_{False}), p(\theta_{True}), p(\theta_{unknown})\} = \{0.1694, 0.8306, 0.0000\}$.